IMPROVING THE SPURIOUS PERFORMANCE OF A DIGITISED ARRAY RECEIVER

F. Rice, L. B. White, Senior Member IEEE and A. Massie *

Cooperative Research Center for Sensor Signal and Information Processing,
Department of of Electrical and Electronic Engineering, Adelaide University, Australia

ABSTRACT

This paper presents the improvement of the spurious free dynamic range (SFDR) for digitisation using antenna arrays. Nonlinearities in the analogue-to-digital conversion degrade the overall SFDR of the digitisation process. We show that array processing, ie, the use of multiple sensors such as antennas or hydrophones with appropriate signal processing can improve the resulting SFDR at the beamform output. By taking advantage of spatial-temporal aliasing and the invisible regions, significant improvements can be obtained using linear, or more effectively, optimal beamforming.

1. INTRODUCTION

This paper in concerned with a perhaps not as widely understood, yet beneficial effect of using sensor arrays when viewed from the point of view of signal digitisation. The analogue-to-digital conversion process is inherently a nonlinear operation, the deficiencies of practical devices and the deleterious effects caused the signal distortion have been studied by many including [5, 1]. These non-idealities in the analogue-to-digital conversion process can degrade the receiver sensitivity due primarily to the production of intermodulation distortion components which limit the useful dynamic range of the analogue-to-digital converter (ADC) [4], resulting in a drop in overall system performance. Antenna arrays suffer the same problem [3] with distortion since for digital beamforming, an ADC is used to first digitise the signals from each array sensor. Early research results have revealed that the linear beamformer has low capacities to cope with ADC nonlinearities [1] and [2]. However, in the case of a digitising array as shown in Figure 1, spurious signals introduced by the ADC appear at a different location in the frequency-wavenumber space to the desired component [4]. This property has motivated us to investigate spatial filters (beamformers) which may remove and/or suppress these undesirable byproducts of the nonideal ADC behaviour. Our measure of the fidelity of the process will be the spurious free dynamic range (SFDR) at the output of the beamformer.

In Section 2, we present the signal processing model used for analysis. Section 3 explains the principles of spatial-temporal filtering, which be used to suppress distortion products and improve the SFDR. The ADC non-linear model is described in Section 4 and a Fourier series representation for the ADC output for a narrowband input is derived. This series representation permits an analytic calculation of the SFDR improvement which can be gained due to the spatial filtering. We discuss optimal beamforming in section 5 and simulation results using multiple input signals are presented in Section 6. We believe that this work represents the first attempt to exploit the spatio-temporal properties of the ADC distortion products by spatial filtering (beamforming) in order to improve overall SFDR.

A. Massie is with Communications Division, Defence Science and Technology Organisation, Salisbury SA, Australia

2. SIGNAL PROCESSING MODEL

Figure 1 shows the signal processing model under study. Each array sensor signal is passed through an analogue anti-aliasing filter with cutoff frequency of $f_s/2$ where f_s is the ADC sampling rate. The sampled signals at the ADC output are then quadrature downmixed with local oscillator frequency f_o, and low-pass filtered using a digital filter with transfer function $H(f)$. These complex baseband signals from each sensor are then combined using a beamformer.

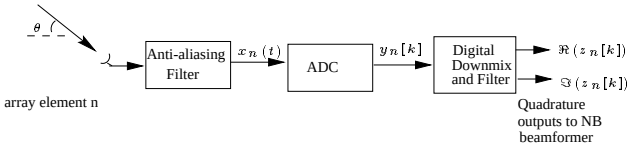

Fig. 1. Signal processing model for array digitisation

For simplicity, we restrict attention to linear, equispaced arrays. We consider an array with N isotropic sensors each separated by d metres. The response at sensor n to a single narrowband plane wave incident at wavenumber ν with carrier frequency f Hz is

$$x_n(t) = \Re\left(s(t)\, e^{i2\pi f(t+n\nu d/c)}\right) , \qquad (1)$$

where $s(t)$ is the baseband modulation on the signal and c denotes the wave propagation speed in m/s, In the paper, we will assume continuous wave modulation with $s(t) = A$ for some constant $A > 0$.

Each sensor signal is passed through an identical ADC, which we represent by the operator $\mathcal{H}$. We will discuss a typical models for the ADC process in section 4. The sample rate is given by f_s Hz. The output of the ADC for sensor n is

$$y_n[k] = \mathcal{H}(x_n)(k/f_s) , \qquad (2)$$

for $k \geq 0$. Each signal is quadrature downmixed with oscillator frequency f_0, and (low-pass) filter impulse response coefficients $h[k], k \geq 0$, yielding

$$z_n[k] = \sum_{\ell \geq 0} h[\ell]\, y_n[k-\ell]\, e^{-2\pi i(k-\ell) f_0/f_s} . \qquad (3)$$

These signals are combined using a beamformer

$$z[k] = \sum_{n=0}^{N-1} g_n(f_0\nu_0)\, z_n[k], \tag{4}$$

where g_n are the beamformer weights. Here ν_0 is the wavenumber of the desired signal. For a conventional linear beamformer we have

$$g_n(\beta) = w_n\, e^{-2\pi i n \beta d/c}, \tag{5}$$

where the $w_n, n = 0, \ldots, N-1$ are real windowing (or shading) coefficients chosen to tradeoff main lobe width and side lobe levels. It is often useful to define the *spatial-temporal array response*

$$W(\beta) = \sum_{n=0}^{N-1} w_n\, e^{-2\pi i n \beta d/c} \tag{6}$$

which is a periodic function with period c/d. Figure 2 shows the array responses for a $N = 10$ element array with $d = 10$m, $T = 1000$ samples and $w_n = 1/N$ for the linear beamforming and the optimum beamforming response which we discuss in Section 5. Notice that the beamformer response is a function of the product $\beta = f_o\,\nu_o$ of the frequency and spatial frequency. It is this property that we exploit in order to improve the SFDR at the output.

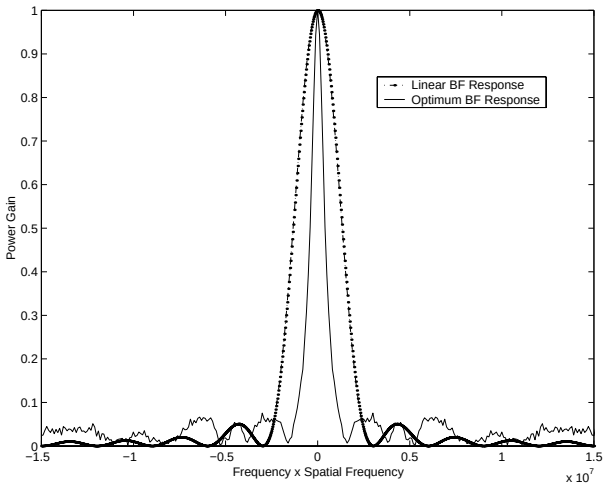

Fig. 2. Beamforming responses

Consider the case where the ADC process is ideal, i.e. $\mathcal{H}$ is the identity operator, and $s(t) = A$. Then from (1) to (5) we obtain

$$\begin{aligned} z[k] &= \sum_{n=0}^{N-1} \sum_{\ell \geq 0} h[\ell]\, w_n\, e^{-i2\pi f_0((k-\ell)/f_s + n\nu_0 d/c)} \\ &\qquad A\, \Re[e^{i2\pi f((k-\ell)/f_s + n\nu d/c)}] \\ &= \frac{A}{2} \sum_{n=0}^{N-1} \sum_{\ell \geq 0} h[\ell]\, w_n \Big[e^{-i2\pi(f_0-f)(k-\ell)/f_s} \\ &\quad e^{-i2\pi n d/c(f_0\nu_0 - f\nu)} + e^{-i2\pi(f_0+f)(k-\ell)/f_s}\, e^{-i2\pi n d/c(f_0\nu_0 + f\nu)} \Big] \end{aligned} \tag{7}$$

Thus

$$\begin{aligned} z[k] &= \frac{A}{2}\Big[e^{-i2\pi(f_0-f)k/f_s} H(f-f_0) W(f_0\nu_0 - f\nu) \\ &\quad + e^{-i2\pi(f+f_0)k/f_s} H(-f-f_0) W(f_0\nu_0 + f\nu) \Big] \end{aligned} \tag{8}$$

If the incident signal was indeed the desired signal, then we set $f_0 = f$ and $\nu_0 = \nu$, yielding

$$z[k] = \frac{A}{2}\left[H(0)W(0) + e^{-i4\pi f k/f_s} H(-2f) W(2f\nu) \right]. \tag{9}$$

Typically, the low pass filter cutoff is chosen so that $H(-2f)$ is negligible, and we scale the low-pass filter ($h[k]$) and beamformer (w_n) coefficients so that $H(0) = 2$ and $W(0) = 1$, thus yielding unit response to the desired signal.

3. SPATIAL-TEMPORAL ALIASING

As pointed out earlier, we process the received array signals in both the temporal and spatial domain. The temporal sampling is performed at rate f_s, so temporal aliasing will occur with period f_s. Spatial sampling is performed by the sensor array, with spatial aliasing occurring with spatio-temporal (ie in the product $\beta = f\nu$) period c/d. When the harmonic signal terms have frequency or spatio-temporal product β which exceeds half the relevant sample rate, they are folded back in the fundamental region. Figure 3 illustrates the aliasing and the invisible regions (for positive temporal frequencies only). Here f_c is the cutoff frequency of the (digital) low pass filter. The visible region is defined to be those that correspond to $-1 \leq \sin\theta \leq 1$. The dashed line with wavenumber $\nu = \pm 1$ shown as OA and OB splits the spatial-temporal representation into two regions - visible region and invisible region. The invisible region has spatial frequencies which do not correspond to any physically valid arrival angle on the array, however as we shall see, distortion terms from the ADC can fall in this region.

4. NONLINEAR ADC MODEL

In this section, we derive a Fourier series representation for the ADC output when the input is a single narrowband signal. This representation is useful for determining the SFDR improvement analytically. All ADCs possess non-linearities due to the non-ideal sample, hold operation and amplifier non-linearities. Considering a sample-and-hold with input-dependent timing jitter we have a ADC non-linear model as below [5]

$$f[x(t)] = x(t) + \gamma \dot{x}(t)\,[M - |x(t)|]\,. \tag{10}$$

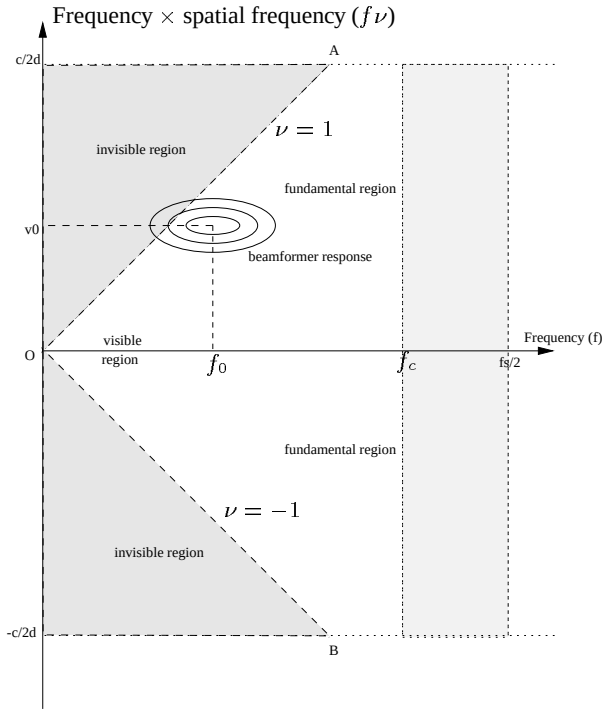

Fig. 3. Spatio-temporal aliasing and the invisible regions

where M is the maximum modulus of $x(t)$, γ is a measure of the departure from linearity, and $\dot{x}$ denotes the derivative of x. This model is desirable since it does not depend explicitly on the type or parameters associated with the signal.

For narrowband inputs (i.e. sinusoids), the output consists of a harmonic series of sinusoids at multiples of the input frequency. In general, for input $x_n(t) = A\cos(2\pi f(t+\tau_n))$, the ADC output is given as

$$\begin{aligned} f[A\cos(2\pi f(t+\tau_n))] &= A\cos(2\pi f(t+\tau_n)) \\ &-2\pi f A^2\gamma\sin(2\pi f(t+\tau_n))\,(1-|\cos(2\pi f(t+\tau_n)|) \end{aligned} \quad (11)$$

The output of the ADC is

$$\begin{aligned} y_n(t) &= A\cos(2\pi ft) - 2\pi\gamma f A^2\delta_1\sin(2\pi ft) \\ &\quad -2\pi\gamma f A^2\sum_{k=2}^{\infty}\delta_k\ \sin(2\pi ft(2k-1))\,, \end{aligned} \quad (12)$$

where the δ_k terms are defined in the appendix. This permits SFDR expressions to be obtained at the input and output of the beamformer. In section 6, we present a comparison between these theoretical expressions and simulation results.

5. OPTIMAL BEAMFORMING

The Minimum Variance Distortionless Response (MVDR) beamformer is an optimal approach to the beamforming problem. The objective is to use the output of the quadrature downmix to specify the beamformer weights g_n. Assume the carrier frequency f and the wavenumber ν, an element of the array steering vector is

$$\mu_n(\beta) = e^{2\pi i dn\beta/c}, \qquad n = 0, 1, \ldots N-1. \quad (13)$$

We choose g_n by fixing the gain as unity for desired $\beta = f_0\nu_0$ and minimising the total output power. The solution for the weight vector $g = [g_0, \ldots, g_{N-1}]^T$ is given by

$$g = \frac{R_z^{-1}\mu(f_0\nu_0)}{\mu^H(f_0\nu_0)R_z^{-1}\mu(f_0\nu_0)}. \quad (14)$$

where R_z is the estimated $N \times N$ array data (after ADC and the down-conversion) covariance matrix

$$[R_z]_{nm} = \frac{1}{T}\sum_{k=1}^{T} z_n[k]\, z_m^*[k]\,, \quad (15)$$

for some block of data of length of T samples. Here ^{H} denotes conjugate transpose and * denotes conjugation. The optimum beamforming response is plotted in Figure 2, together with the linear beamforming response. The optimum array response is much sharper than the linear one, although sidelobes are higher in this particular example.

6. EXPERIMENTAL RESULTS

We wish to compare the effect of the beamforming operation in terms of suppression of undesirable signal components introduced by the ADC nonidealities. We will assume that the quadrature downmix local oscillator frequency f_o is set to the carrier frequency of the desired signal, and that the beamformer parameter β is set to the product $f_o\nu_o$ of the desired signal carrier frequency and wavenumber. The SFDR will be defined as the ratio of the power of the desired signal component to the power of the next largest term at the beamformer output when all signals have equal power. Clearly this will depend on the bandwidth of the low pass filter $H(f)$. In practice, one would set the bandwidth of H suitably small to cover just the passband of the signal of interest. We shall set the bandwidth of H variously between 0.10 and 0.35 of the sampling frequency f_s in our experiments in order to illustrate the benefits of our approach. This is still a realistic situation since in a very dense signal environment such as is found in the HF bands, there still remains a high probability of distortion products appearing in the chosen passband.

Consider a single incident on a uniform linear array with 10 elements and the array spacing $d = 10$ m. We assume that the baseband transmitted signal is a constant $s(t) = 1$, with carrier frequency $f_0 = 10$ MHz, the arrival angle $\theta = \frac{\pi}{6}$, the sample rate $f_s = 36$ MHz and the anti-aliasing filter cutoff frequency $f_c = 0.35\, f_s$. Aliased harmonics are shown in Table 1 together with the comparison of the calculated SFDR (using the Fourier series representation) and simulated results.

Table 1 shows a good agreement between the theoretical calculation and the simulated results. The 3rd order term is located on the border of the invisible region. The linear beamforming increases SFDR over 10 dB in both measurements. The simulation results also show that the performance of the optimum beamformer is similar to that of the linear beamformer.

Multiple incidents signals were simulated with carrier frequencies $f_1 = 7$ MHz, $f_2 = 10$ MHz and $f_3 = 13$ MHz and corresponding arrival angles $\theta_1 = \frac{\pi}{4}, \theta_2 = \frac{\pi}{3}$ and $\theta_3 = \frac{\pi}{9}$. Each carrier

Signal Components	Signal	Harmonics		
	1	3	5	7
Frequency (MHz) - f	10	-6	14	-2
$\beta = f\nu$	5	15	-5	5
Location	Visible	Invisible	Visible	Visible
Theoretical SFDR (dB)				
Before Beamforming	0	-35.9	-48.4	-58.4
Linear Beamforming	0	-51.2	-63.6	-74.1
Simulated SFDR (dB)				
Before Beamforming	0	-36.2	-49.8	-59.4
Linear Beamforming	0	-50.9	-60.0	-79.4

Table 1. SFDR improvement for a single signal

had unit amplitude. The sample rate f_s was 36 MHz and the anti-aliasing filter cutoff frequency was $0.1\,f_s$. The linear equispaced array has 10 elements and array spacing $d = 10m$. We assumed that the ADC non-linearity factor was $\gamma = 10^{-10}$. The desired signal was at $f_0 = 10$ MHz with the arrival angle $\theta = \frac{\pi}{3}$. Complex additive white Gaussian noise was added to the signal at SNR = 9 dB.

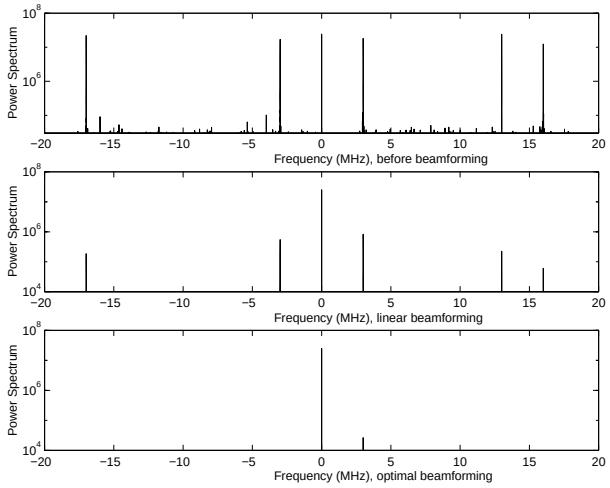

Fig. 4. Power spectra before beamforming and after linear and optimal beamforming

Figure 4 shows the power spectrum of one sensor signal before beamforming, and the power spectrum of the beamformer outputs, both linear and optimal. The SFDR is -0.25 dB before the any beamforming, SFDR = 14.86 dB for the linear beamformer output and SFDR = 30.32 dB for the optimum beamformer output. The performance of the optimum beamformer is superior to that of the linear beamformer by around 10 dB. We then varied the desired arrival direction ν_o only and kept other parameters unchanged. The simulation results are shown in Figure 5. A clear degradation is evident in the region around $\nu_0 = 0.48$ corresponding to $\beta = 4.8 \times 10^6$. This degradation is due to the presence of the fundamental components of the other 2 signals at $f\nu = 4.94 \times 10^6,\ 4.45 \times 10^6$. The optimal beamformer appears to maximise SFDR at the desired $f\nu = 0.866 \times 10^6$.

7. CONCLUSION

We have investigated the applicability of sensor array processing in improving the spurious free dynamic range of the resulting digi-

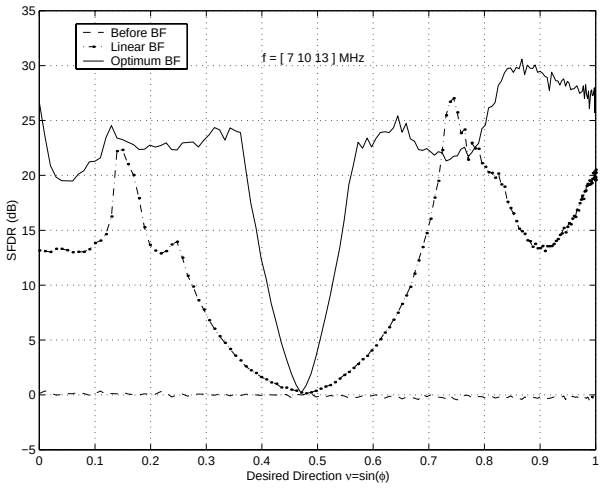

Fig. 5. Comparison of performance of the beamformers for three incident signals

tised signal. We have demonstrated that significant suppression of spurious terms produced by nonidealities in the signal digitisation process can be obtained by exploiting both their spatial and temporal frequency properties. Spatio-temporal filtering suppresses undesired spurious terms introduced by the imperfections in the analogue-to-digital conversion process since these terms are generally found in different locations in the spatio-temporal co-ordinate space than the desired signals. Simulation results have compared the performance of the linear beamformer and the minimum variance distortionless response beamformer in terms of spurious free dynamic range (SFDR) improvement. These results indicate that the MVDR beamformer has superior performance to the linear beamformer, and that the MVDR beamformer appears to optimise SFDR for the desired signal of interest.

8. REFERENCES

[1] D.R. Ucci and R. G. Petriot, "The effects of ADC Nonlinearities on Digital Beamformers, " *Military Communications Conference, 1989. MILCOM '89. Conference Record, Bridging the Gap, Interoperability, Survivability, Security" 1989 IEEE, 1989*, page(s) : 279 -283 vol, 1.

[2] J. Litva and T.K. Lo, "Digital Beamforming in Wireless Communications", *Artech House Publishers*, 1996.

[3] S. L. Loyka, "The influence of electromagnetic environment on operation of active array antennas: analysis and simulation techniques," *Antennas and Propagation Magazine*, vol. 41, No. 6, pp. 23–39, December 1999.

[4] A. Massie and D. Taylor and J. Kitchen and L. Casey and W. Marwood, "Enhancing the performance of direct digitising arrays with super-resolution and co-channel techniques," *Communication Division*, DSTO, 1999

[5] J. Tsimbinos and K. Lever, "Applications of higher-order statistics to modelling, identification and cancellation of nonlinear distortion in high-speed samplers and analogue-to-digital converters using the Volterra and Wiener models' *IEEE Signal Processing Workshop on Higher Order Statistics*, pp. 379–383, South Lake Tahoe, CA, USA, 1993.